




MUSCLE: Multi-task Self-supervised Continual Learning to Pre-train Deep Models for X-Ray Images of Multiple Body Parts

Weibin Liao¹, Haoyi Xiong¹ , Qingzhong Wang¹, Yan Mo¹, Xuhong Li¹, Yi Liu¹, Zeyu Chen¹, Siyu Huang², and Dejing Dou¹

¹ Baidu, Inc., Beijing, China
xionghaoyi@baidu.com

² Harvard University, Cambridge, MA, USA

Abstract. While self-supervised learning (SSL) algorithms have been widely used to pre-train deep models, few efforts [11] have been done to improve representation learning of X-ray image analysis with SSL pre-trained models. In this work, we study a novel self-supervised pre-training pipeline, namely *Multi-task Self-supervised Continual Learning* (MUSCLE), for multiple medical imaging tasks, such as classification and segmentation, using X-ray images collected from multiple body parts, including heads, lungs, and bones. Specifically, MUSCLE aggregates X-rays collected from multiple body parts for MoCo-based representation learning, and adopts a well-designed continual learning (CL) procedure to further pre-train the backbone subject various X-ray analysis tasks jointly. Certain strategies for image pre-processing, learning schedules, and regularization have been used to solve *data heterogeneity*, *overfitting*, and *catastrophic forgetting* problems for multi-task/dataset learning in MUSCLE. We evaluate MUSCLE using 9 real-world X-ray datasets with various tasks, including pneumonia classification, skeletal abnormality classification, lung segmentation, and tuberculosis (TB) detection. Comparisons against other pre-trained models [7] confirm the *proof-of-concept* that self-supervised multi-task/dataset continual pre-training could boost the performance of X-ray image analysis.

Keywords: X-ray images (X-ray) · Self-supervised learning

1 Introduction

While deep learning-based solutions [1] have achieved great success in medical image analysis, such as X-ray image classification and segmentation tasks for

Supplementary Information The online version contains supplementary material available at https://doi.org/10.1007/978-3-031-16452-1_15.

diseases in bones, lungs and heads, it might require an extremely large number of images with fine annotations to train the deep neural network (DNN) models and deliver decent performance [2] in a supervised learning manner. To lower the sample size required, the self-supervised learning (SSL) paradigm has been recently proposed to boost the performance of DNN models through learning visual features from images [3] without using labels.

Among a wide range of SSL methods, contrastive learning [4] algorithms use a similarity-based metric to measure the distance between two embeddings derived from two different views of a single image, where the views of image are generated through data augmentation, e.g., rotation, clip, and shift, and embeddings are extracted from the DNN with learnable parameters. In particular, for computer vision tasks, the contrastive loss is computed using the feature representations of the images extracted from the encoder network, resulting in the clustering of similar samples together and the dispersal of different samples. Recent methods such as SwAV [5], SimCLR [6], MoCo [7], and PILR [8] have been proposed to outperform supervised learning methods on natural images. While contrastive learning methods have demonstrated promising results on natural image classification tasks, the attempts to leverage them in medical image analysis are often limited [9, 10]. While Sowrirajan et al. [11] proposed MoCo-CXR that can produce models with better representations for the detection of pathologies in chest X-rays using MoCo [7], the superiority of SSL for *other X-ray analysis tasks, such as detection and segmentation, on various body parts, such as lung and bones, is not yet known.*

Our Contributions. In this work, we proposed MUSCLE-*M*ulti-task *S*elf-supervised *C*ontinual *L*earning (shown in Fig. 1) that pre-trains deep models using X-ray images collected from multiple body parts subject to various tasks, and made contributions as follow.

1. We study the problem of multi-dataset/multi-task SSL for X-ray images. To best of our knowledge, only few works have been done in related area [11, 12], especially by addressing *data heterogeneity* (e.g., image sizes, resolutions, and gray-scale distributions), *over-fitting* (e.g., to any one of the tasks), and *catastrophic forgetting* (e.g., ejection of knowledge learned previously) in multi-dataset/multi-task learning settings.
2. We present MUSCLE that pre-trains the backbone in multi-dataset/multi-task learning settings with task-specific heads, including Fully-Connected (FC) Layer, DeepLab-V3 [13], and FasterRCNN [14] for classification, segmentation, and abnormal detection tasks respectively. As shown in Fig. 1, MUSCLE (1) adopts MoCo to learn representations with a backbone network from multiple datasets, with pre-processing to tackle *data heterogeneity*, and further (2) pre-trains the backbone to learn discriminative features with continual learning (CL) subject to multiple tasks, while avoiding over-fitting and “catastrophic forgetting” [15, 16]. MUSCLE finally (3) fine-tunes the pre-trained backbone to adapt every task independently and separately.

3. In this work, we collect 9 X-ray datasets to evaluate MUSCLE, where we pre-train and fine-tune the network to adapt all tasks using training subsets, and validate the performance using testing subsets. The experimental results show MUSCLE outperforms ImageNet/MoCo pre-trained backbones [11] using both ResNet-18 and ResNet-50 as backbones. The comparisons confirm the *proof-of-concept* of MUSCLE—self-supervised multi-task/dataset continual pre-training can boost performance of X-ray image analysis.

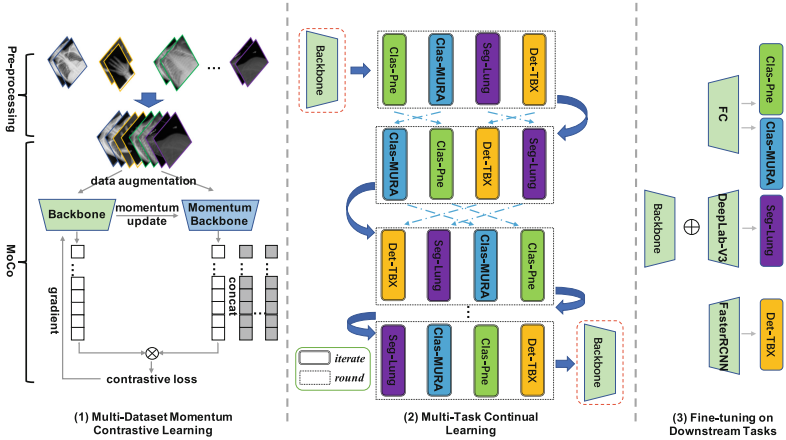


Fig. 1. The pipeline of MUSCLE, consists of three parts (1) Multi-Dataset Momentum Contrastive (Multi-Dataset MoCo) Learning, (2) Multi-Task Continual Learning and (3) Fine-tuning on Downstream Tasks.

2 Methodologies

In this section, we present the framework and algorithms design for MUSCLE. As was shown in Fig. 1, MUSCLE consists of three steps as follows.

1. *Multi-dataset momentum contrastive learning.* (MD-MoCo) Give multiple datasets of X-ray images collected from different body parts and based on different image resolution and gray-scale distributions, MUSCLE aggregates these datasets with pre-processing (e.g., resize, re-scale, and normalization), then adopts a MoCo-based SSL algorithm [11] to pre-train the backbone networks and learn the representation of X-ray images within the aggregated dataset.
2. *Multi-task continual learning.* Given the MD-MoCo pre-trained backbone and the datasets for different X-ray analysis tasks, e.g., pneumonia classification, skeletal abnormality classification, and lung segmentation, MUSCLE leverages continual learning algorithms and further pre-trains a unified backbone network with alternating heads to learn the various sets of discriminative features subject to the different tasks.

3. *Fine-tuning with downstream tasks.* Given the pre-trained backbone and every downstream X-ray image analysis task, MUSCLE fine-tunes and outputs a neural network using pre-trained weights as the initialization and its own task-specific head to fit the task independently.

2.1 Multi-Dataset Momentum Contrastive Learning (MD-MoCo)

To pre-train the backbone with multiple datasets, MUSCLE collects and aggregates nine X-ray image datasets listed in Table 1. While these datasets have offered nearly 179,000 X-ray images covering cover several parts of the human body, including the chest, hand, elbow, finger, forearm, humerus, shoulder and wrist, MUSCLE makes non-trivial extension to adopt MoCo [4, 11] for *multi-dataset momentum contrastive learning* as follows.

Table 1. An overview of nine publicly available X-ray image datasets

Datasets	Body part	Task	Train	Valid	Test	Total
Only Used for the first step (MD-MoCo) of MUSCLE						
NIHCC [17]	Chest	N/A	112,120	N/A	N/A	112,120
China-Set-CXR [18]	Chest	N/A	661	N/A	N/A	661
Montgomery-Set-CXR [18]	Chest	N/A	138	N/A	N/A	138
Indiana-CXR [19]	Chest	N/A	7,470	N/A	N/A	7,470
RSNA Bone Age [20]	Hand	N/A	10,811	N/A	N/A	10,811
Used for all three steps of MUSCLE						
Pneumonia [21]	Chest	Classification	4,686	585	585	5,856
MURA [22]	Various Bones	Classification	32,013	3,997	3,995	40,005
Chest Xray Masks [18]	Chest	Segmentation	718	89	89	896
TBX [23]	Chest	Detection	640	80	80	800
Total	N/A	N/A	169,257	4,751	4,749	178,757

Re-sizing, Re-scaling, Normalization, and Aggregation. The major challenge to work with multiple X-ray image datasets collected from different body part is the heterogeneity of images, including X-ray image resolutions and the distribution of gray-scales. To aggregate these datasets, several image pre-processing schemes have been used, where MUSCLE transforms and normalizes the gray-scale distribution of these datasets using the Z-score method with the mean of 122.786 and a standard deviation of 18.390. Further to fully utilize GPU for the resource-consuming MoCo algorithms, MUSCLE re-sizes all images into a 800×500 resolution which balances the effectiveness and efficiency of deep learning.

MoCo-Based Pre-training with Aggregated Datasets. To utilize MoCo algorithm [4] for X-ray images pre-training, MUSCLE further extends MoCo-CXR [11] with advanced settings on data augmentation strategies and initialization tricks. Specifically, while MoCo uses random data augmentation to generate contrastive

views, MUSCLE disables random cropping, gaussian blurring, color/gray-scale jittering to preserve the semantic information for medical images. Furthermore, MUSCLE initializes the MoCo-based pre-training procedure with Kaiming’s initialization [24] to setup the convolution layers, so as to ensure the stability of back-propagation in contrastive learning.

Note that, in this work, the training sets of all nine datasets have been used for *multi-dataset momentum contrastive learning*, while four of them with specific X-ray image analysis tasks are further used for *multi-task continual learning*.

2.2 Multi-task Continual Learning

To further pre-train the backbone subject to task-specific representations, MUSCLE adopts the continual learning (CL) [25] with four X-ray image analysis tasks, including pneumonia classification from Pneumonia [21], skeletal abnormality classification from MURA [22], lung segmentation from Chest Xray Masks and Labels [18], and Tuberculosis(TB) detection from TBX [23]. Specifically, MUSCLE extends the vanilla CL for neural network, which iterates the training procedures of the backbone network with alternating task-specific heads subject to tasks, with two major advancements as follows.

Cyclic and Reshuffled Learning Schedule. MUSCLE splits the continual learning procedure into 10 **rounds** of learning process, where each round of learning process **iterates** the 4 learning tasks one-by-one and each iterate of learning task trains the backbone network with 1 epoch using a task-specific head, i.e., Fully-Connected (FC) Layer for classification tasks, DeepLab-V3 [13] for segmentation tasks, and FasterRCNN [14] for detection tasks. Furthermore, to avoid overfitting to any task, MUSCLE reshuffle the order of tasks in every round of learning process, and adopts Cosine annealing learning rate schedule as follow.

$$\eta_t = \eta_{\min}^i + \frac{1}{2} (\eta_{\max} - \eta_{\min}) \left(1 + \cos \left(\frac{t}{T} \cdot 2\pi \right) \right) \quad (1)$$

where η_t refers to the learning rate of the t^{th} iteration, η_{\max} and η_{\min} and T_i refer to the maximal and minimal learning rates, and T refers to the total number of iterations within a period of cyclic learning rate schedule.

Cross-Task Memorization with Explicit Bias. Yet another challenge of multi-task CL is “catastrophic forgetting”, where the backbone would “forget” the knowledge learned from the previous iterates. To solve the problem, MUSCLE leverages a knowledge transfer regularization derived from L²-SP [15]. In each iterate of learning task, given the pre-trained model obtained from previous iterates, MUSCLE sets the pre-trained weights as \mathbf{w}_S^0 and trains the backbone using the following loss, where \mathbf{w}_S is the learning outcome and α is the hyper-parameter.

$$\Omega(\mathbf{w}_S) = \underbrace{\alpha \left\| \mathbf{w}_S - \mathbf{w}_S^0 \right\|_2^2}_{\substack{\text{distance to the model} \\ \text{pre-trained by previous iterates.}}} + \underbrace{(1 - \alpha) \left\| \mathbf{w}_S \right\|_2^2}_{\substack{\text{Ridge-based} \\ \text{regularization.}}} \quad (2)$$

outcome of CL
pre-trained by previous iterates

Thus, above regularization constrains the distance between the learning outcome and the backbone trained by the previous iterates.

2.3 Fine-Tuning on Downstream Tasks

Finally, given the backbone pre-trained using above two steps, MUSCLE fine-tunes the backbone on each of the four tasks independent and separately. Again, MUSCLE connects the pre-trained backbone with Fully-Connected (FC) Layer for classification tasks, DeepLab-V3 [13] for segmentation tasks, and Faster-RCNN [14] for detection tasks. Finally, MUSCLE employs the standard settings, such as vanilla weight decay as stability regularization and step-based decay of learning rate schedule, for such fine-tuning.

Table 2. Performance comparisons for pneumonia classification (pneumonia) and skeletal abnormality classification (MURA) using various pre-training algorithms.

Datasets	Backbones	Pre-train	Acc.	Sen.	Spe.	AUC (95%CI)
Pneumonia	ResNet-18	Scratch	91.11	93.91	83.54	96.58 (95.09–97.81)
		ImageNet	90.09	93.68	80.38	96.05 (94.24–97.33)
		MD-MoCo	96.58	97.19	94.94	98.48 (97.14–99.30)
		MUSCLE ⁺⁺	96.75	97.66	94.30	99.51 (99.16–99.77)
		MUSCLE	97.26	97.42	96.84	99.61 (99.32–99.83)
	ResNet-50	Scratch	91.45	92.51	88.61	96.55 (95.08–97.82)
		ImageNet	95.38	95.78	94.30	98.72 (98.03–99.33)
		MD-MoCo	97.09	98.83	92.41	99.53 (99.23–99.75)
		MUSCLE ⁺⁺	96.75	98.36	92.41	99.58 (99.30–99.84)
		MUSCLE	98.12	98.36	97.47	99.72 (99.46–99.92)
MURA	ResNet-18	Scratch	81.00	68.17	89.91	86.62 (85.73–87.55)
		ImageNet	81.88	73.49	87.70	88.11 (87.18–89.03)
		MD-MoCo	82.48	72.27	89.57	88.28 (87.28–89.26)
		MUSCLE ⁺⁺	82.45	74.16	88.21	88.41 (87.54–89.26)
		MUSCLE	82.62	74.28	88.42	88.50 (87.46–89.57)
	ResNet-50	Scratch	80.50	65.42	90.97	86.22 (85.22–87.35)
		ImageNet	81.73	68.36	91.01	87.87 (86.85–88.85)
		MD-MoCo	82.35	73.12	88.76	87.89 (87.06–88.88)
		MUSCLE ⁺⁺	81.10	69.03	89.48	87.14 (86.10–88.22)
		MUSCLE	82.60	74.53	88.21	88.37 (87.38–89.32)

3 Experiment

In this section, we present our experimental results to confirm the effectiveness of MUSCLE on various tasks.

Experiment Setups. In this experiments, we include performance comparisons on pneumonia classification (Pneumonia) [21], skeletal abnormality classification (MURA) [22], lung segmentation (Lung) [18], and tuberculosis detection (TBX) [23] tasks. We use the training sets of these datasets/tasks to pre-train and fine-tune the network with MUSCLE or other baseline algorithms, tune the hyper-parameters using validation sets, and report results on testing datasets.

As the goal of MUSCLE is to pre-train backbones under multi-task/dataset settings, we propose several baselines for comparisons as follows. **Scratch**: the models are all initialized using Kaiming’s random initialization [24] and fine-tuned on the target datasets (introduced in Sect. 2.3). **ImageNet**: the models are initialized using the officially-released weights pre-trained by the ImageNet dataset and fine-tuned on the target datasets. **MD-MoCo**: the models are pre-trained using *multi-dataset MoCo* (introduced in Sect. 2.2) and fine-tuned accordingly; we believe MD-MoCo is one of our proposed methods and can prove the concepts,

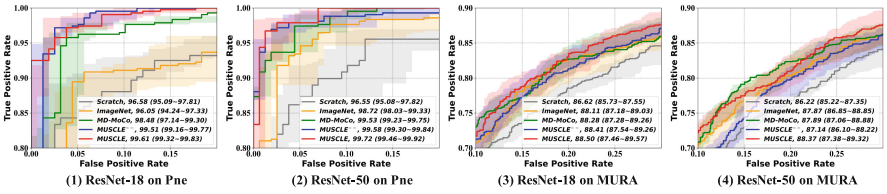


Fig. 2. Receiver Operating Characteristic (ROC) Curves with AUC value (95%CI) on pneumonia classification (Pne) and skeletal abnormality classification (MURA)

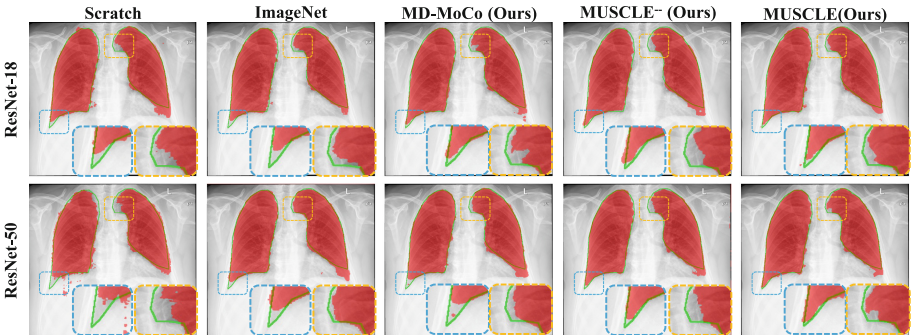


Fig. 3. Results using various pre-training algorithms on lung segmentation, where green lines indicate ground truth and red areas indicate model prediction results, and the blue and orange boxes cover regions of the main differences in these results. (Color figure online)

as MD-MoCo extends both vanilla MoCo [7] and MoCo-CXR [11] with additional data pre-processing methods to tackle the multi-dataset issues. MUSCLE⁻⁻: all models are pre-trained and fine-tuned with MUSCLE but with *Cross-Task Memorization* and *Cyclic and Reshuffled Learning Schedule* turned off. All models here are built with ResNet-18 and ResNet-50.

To compare these algorithms, we evaluate and compare *Accuracy* (Acc.), *Area under the Curve* (AUC), *Sensitivity* (Sen.), *Specificity* (Sep.) and *Receiver Operating Characteristic (ROC) Curve* for Pneumonia and MURA classification tasks, *Dice Similarity Coefficient* (Dice), *mean Intersection over Union* (mIoU) for lung segmentation (Lung) task, and *mean Average Precision* (mAP), *Average Precision of Active TB* (AP_{active}) and *Average Precision of Latent TB* (AP_{latent}) for tuberculosis detection (TBX), all of them at the IoU threshold of 0.5. AUC values are reported with 95% confidence intervals estimated through bootstrapping with 100 independent trials on testing sets.

Overall Comparisons. We present the results on Pneumonia and MURA classification tasks in Table 2 and Fig. 2, where we compare the performance of MUSCLE with all baseline algorithms and plot the ROC curve. Results show that our proposed methods, including MUSCLE, MUSCLE⁻⁻ and MD-MoCo can significantly outperform the one based on ImageNet pre-trained models and Scratch. Furthermore, in terms of overall accuracy (Acc. and AUC), MUSCLE outperforms MD-MoCo and MUSCLE⁻⁻ in all cases, due to its advanced continual learning settings. However, we can still observe a slightly lower sensitivity on the Pneumonia classification task and a slightly lower specificity on the MURA delivered by MUSCLE. Similar observations could be found in Table 3 and Fig. 3, where we report the performance on lung segmentation and TB detection tasks with examples of lung segmentation plotted.

More Comparisons. Please note that MD-MoCo indeed surpasses **MoCo** [7] and **MoCo-CXR** [11] (state of the art in X-rays pre-training), in terms of performance, as it uses multiple datasets for pre-training and solves the data heterogeneity problem (the performance of MoCo might be even worse than ImageNet-based pre-training, if we don't unify the gray-scale distributions of X-ray images collected from different datasets). We also have tried to replace MoCo with **SimCLR** [6], the performance of SimCLR for X-ray pre-training is even worse, e.g., 87.52% (9.57%↓) Acc. for pneumonia classification.

Furthermore, though MUSCLE is proposed as a “*proof-of-concept*” solution and has not been optimized for any single medical imaging task, e.g., using U-Net for segmentation [26], the overall performance of MUSCLE is still better than many recent works based on the same datasets. For example, *Stephen et al. (2019)* [27] reports a 93.73% (4.42%↓) accuracy for the same pneumonia classification task and *Li et al. (2021)* [28] reports a 94.64% Dice (0.73%↓) for the lung segmentation. For MURA, *Bozorgtabar et al. (2020)* [29] reports an AUC of 82.45% (6.05%↓), while *Liu et al. (2020)* [23] reports a 58.70% (4.76%↓) AP_{active} and a 9.60% (2.61%↓) AP_{latent} for TBX based on FasterRNN. The advantages of MUSCLE demonstrate the feasibility of using multiple tasks/datasets to pre-train the backbone with SSL and CL. For more results, please refer to the appendix.

Ablation Studies. The comparisons between Scratch versus MD-MoCo, between MD-MoCo versus MUSCLE⁻⁻, and between MUSCLE⁻⁻ versus MUSCLE confirm the contributions made by each step of our algorithms. Frankly speaking, in many cases, MD-MoCo achieved the most performance improvement (compared to ImageNet or Scratch), while continual learning without *Cyclic & Reshuffled Learning Schedule* and *Cross-Task Memorization* may even make MUSCLE⁻⁻ performs worse, due to over-fitting or catastrophic forgetting. However, MUSCLE, pipelining MD-MoCo and advanced continual learning strategies, successfully defends her dominant position and outperforms other algorithms in most cases.

Table 3. Performance comparisons for lung segmentation (lung) and TB Detection (TBX) using various pre-training algorithms.

Backbones	Pre-train	Lung		TBX		
		Dice	mIoU	mAP	AP _{Active}	AP _{Latent}
ResNet-18	Scratch	95.24	94.00	30.71	56.71	4.72
	ImageNet	95.26	94.10	29.46	56.27	2.66
	MD-MoCo	95.31	94.14	36.00	67.17	4.84
	MUSCLE ⁻⁻	95.14	93.90	34.70	63.43	5.97
	MUSCLE	95.37	94.22	36.71	64.84	8.59
ResNet-50	Scratch	93.52	92.03	23.93	44.85	3.01
	ImageNet	93.77	92.43	35.61	58.81	12.42
	MD-MoCo	94.33	93.04	36.78	64.37	9.18
	MUSCLE ⁻⁻	95.04	93.82	35.14	57.32	12.97
	MUSCLE	95.27	94.10	37.83	63.46	12.21

4 Discussion and Conclusion

In this work, we present MUSCLE a self-supervised continual learning pipeline that pre-trains deep neural networks using multiple X-ray image datasets collected from different body parts, e.g., hands, chests, bones and etc., for multiple X-ray analysis tasks, e.g., TB detection, lung segmentation, and skeletal abnormality classification. MUSCLE proposes *multi-dataset momentum contrastive learning* (MD-MoCo) and *multi-task continual learning* to tackle the data heterogeneity, over-fitting, and catastrophic forgetting problems in pre-training, and finally fine-tunes the network to adapt every task independently and separately. Experiment results on 9 X-ray image datasets show MUSCLE outperforms other pre-training methods, including ImageNet-based and MoCo-based [11] solutions. We do acknowledge that MUSCLE might NOT be an optimized solution for any specific task in this study, we however claim MUSCLE as a “*proof-of-concept*” that demonstrates the feasibility of using multiple datasets/tasks to pre-train X-ray models with advanced strategies of self-supervised continual learning.

References

1. LeCun, Y., Bengio, Y., Hinton, G.: Deep learning. *Nature* **521**(7553), 436–444 (2015)
2. Balki, I., et al.: Sample-size determination methodologies for machine learning in medical imaging research: a systematic review. *Can. Assoc. Radiol. J.* **70**(4), 344–353 (2019)
3. Jing, L., Tian, Y.: Self-supervised visual feature learning with deep neural networks: a survey. *IEEE Trans. Pattern Anal. Mach. Intell.* **43**(11), 4037–4058 (2020)
4. Chen, T., Kornblith, S., Norouzi, M., Hinton, G.: A simple framework for contrastive learning of visual representations. In: *International Conference on Machine Learning*, pp. 1597–1607. PMLR (2020)
5. Caron, M., Misra, I., Mairal, J., Goyal, P., Bojanowski, P., Joulin, A.: Unsupervised learning of visual features by contrasting cluster assignments. In: *Advances in Neural Information Processing Systems*, vol. 33, pp. 9912–9924 (2020)
6. Chen, T., Kornblith, S., Norouzi, M., Hinton, G.: A simple framework for contrastive learning of visual representations. [arXiv:2002.05709](https://arxiv.org/abs/2002.05709) (2020)
7. He, K., Fan, H., Wu, Y., Xie, S., Girshick, R.: Momentum contrast for unsupervised visual representation learning. In: *Proceedings of the IEEE/CVF Conference on Computer Vision and Pattern Recognition*, pp. 9729–9738. IEEE (2020)
8. Misra, I., Maaten, L.V.D.: Self-supervised learning of pretext-invariant representations. In: *Proceedings of the IEEE/CVF Conference on Computer Vision and Pattern Recognition*, pp. 6707–6717. IEEE (2020)
9. Maithra, R., Chiyuan, Z., Jon, K., Samy B.: Transfusion: understanding transfer learning for medical imaging. [arXiv:1902.07208](https://arxiv.org/abs/1902.07208) (2019)
10. Cheplygina, V., de Bruijne, M., Pluim, J.P.: Not-so-supervised: a survey of semi-supervised, multi-instance, and transfer learning in medical image analysis. *Med. Image Anal.* **54**, 280–296 (2019)
11. Sowrirajan, H., Yang, J., Ng, A.Y., Rajpurkar, P.: MoCo pretraining improves representation and transferability of chest X-ray models. In: *Medical Imaging with Deep Learning*, pp. 728–744. PMLR (2021)
12. Memmel, M., Gonzalez, C., Mukhopadhyay, A.: Adversarial continual learning for multi-domain hippocampal segmentation. In: Albarqouni, S., et al. (eds.) *DART/FAIR -2021*. LNCS, vol. 12968, pp. 35–45. Springer, Cham (2021). https://doi.org/10.1007/978-3-030-87722-4_4
13. Chen, L.C., Papandreou, G., Schroff, F., Adam, H.: Rethinking atrous convolution for semantic image segmentation. [arXiv:1706.05587](https://arxiv.org/abs/1706.05587) (2017)
14. Girshick, R.: Fast R-CNN. In: *Proceedings of the IEEE International Conference on Computer Vision*, pp. 1440–1448 (2015)
15. Xuhong, L.I., Grandvalet, Y., Davoine, F.: Explicit inductive bias for transfer learning with convolutional networks. In: *International Conference on Machine Learning*, pp. 2825–2834. PMLR (2018)
16. Gotmare, A., Keskar, N.S., Xiong, C., Socher, R.: A closer look at deep learning heuristics: learning rate restarts, warmup and distillation. [arXiv:1810.13243](https://arxiv.org/abs/1810.13243) (2018)
17. Wang, X., Peng, Y., Lu, L., Lu, Z., Bagheri, M., Summers, R.M.: ChestX-ray8: hospital-scale chest X-ray database and benchmarks on weakly-supervised classification and localization of common thorax diseases. In: *Proceedings of the IEEE Conference on Computer Vision and Pattern Recognition*, pp. 2097–2106. IEEE (2017)

18. Jaeger, S., Candemir, S., Antani, S., Wáng, Y.X.J., Lu, P.X., Thoma, G.: Two public chest X-ray datasets for computer-aided screening of pulmonary diseases. *Quant. Imaging Med. Surg.* **4**(6), 475 (2014)
19. Demner-Fushman, D., et al.: Preparing a collection of radiology examinations for distribution and retrieval. *J. Am. Med. Inform. Assoc.* **23**(2), 304–310 (2016)
20. Halabi, S.S., et al.: The RSNA pediatric bone age machine learning challenge. *Radiology* **290**(2), 498–503 (2019)
21. Kermany, D.S., et al.: Identifying medical diagnoses and treatable diseases by image-based deep learning. *Cell* **172**(5), 1122–1131 (2018)
22. Rajpurkar, P., et al.: MURA: large dataset for abnormality detection in musculoskeletal radiographs. [arXiv:1712.06957](https://arxiv.org/abs/1712.06957) (2017)
23. Liu, Y., Wu, Y.H., Ban, Y., Wang, H., Cheng, M.M.: Rethinking computer-aided tuberculosis diagnosis. In: *Proceedings of the IEEE/CVF Conference on Computer Vision and Pattern Recognition*, pp. 2646–2655. IEEE (2020)
24. He, K., Zhang, X., Ren, S., Sun, J.: Delving deep into rectifiers: surpassing human-level performance on ImageNet classification. In: *Proceedings of the IEEE International Conference on Computer Vision*, pp. 1026–1034. IEEE (2015)
25. Parisi, G.I., Kemker, R., Part, J.L., Kanan, C., Wermter, S.: Continual lifelong learning with neural networks: a review. *Neural Netw.* **113**, 54–71 (2019)
26. Ronneberger, O., Fischer, P., Brox, T.: U-Net: convolutional networks for biomedical image segmentation. In: Navab, N., Hornegger, J., Wells, W.M., Frangi, A.F. (eds.) *MICCAI 2015*. LNCS, vol. 9351, pp. 234–241. Springer, Cham (2015). https://doi.org/10.1007/978-3-319-24574-4_28
27. Stephen, O., Sain, M., Maduh, U.J., Jeong, D.U.: An efficient deep learning approach to pneumonia classification in healthcare. *J. Healthc. Eng.* **2019** (2019)
28. Li, D., Yang, J., Kreis, K., Torralba, A., Fidler, S.: Semantic segmentation with generative models: semi-supervised learning and strong out-of-domain generalization. In: *Proceedings of the IEEE/CVF Conference on Computer Vision and Pattern Recognition*, pp. 8300–8311. IEEE (2021)
29. Bozorgtabar, B., Mahapatra, D., Vray, G., Thiran, J.-P.: SALAD: self-supervised aggregation learning for anomaly detection on X-rays. In: Martel, A.L., et al. (eds.) *MICCAI 2020*. LNCS, vol. 12261, pp. 468–478. Springer, Cham (2020). https://doi.org/10.1007/978-3-030-59710-8_46